14th International Symposium on Turbulence and Shear Flow Phenomena (TSFP14)
Heidelberg, Germany, July 28–31, 2026

UNDERSTANDING THE DRAG OF HETEROGENEOUS AND SPARSE BIOFILMS

Rodrigo Vilumbrales-Garcia
Department of Naval Architecture and Marine Engineering
University of Michigan
Ann Arbor, MI, USA
rodrigga@umich.edu

Jon B. Estrada
Department of Mechanical Engineering
University of Michigan
Ann Arbor, MI, USA
jbestrad@umich.edu

Harish Ganesh
Department of Naval Architecture and Marine Engineering
University of Michigan
Ann Arbor, MI, USA
gharish@umich.edu

ABSTRACT

Predicting drag penalties due to biofouling on marine vehicles remains a significant challenge. Several factors, such as types and distributions (coverage) of species, the growth duration, the nature of the resulting fouling morphology (presence of streamers, compliance, etc.), and sloughing with time, make prediction challenging. Studying the individual contribution of such factors using a live fouling in a controlled laboratory setting, is challenging. In this study, the effect of coverage, arrangement, and mechanical properties of synthetic biofilm-like surfaces on skin-friction drag is studied in a turbulent channel flow. The study is informed based on growth and drag produced by live bacterial films observed in the Naval Research Laboratory (NRL) in Key West, Florida, USA. The main objective is to compare the relationship between the measured drag of synthetic heterogeneous surfaces with live fouling and quantify the effect of parameters such as coverage, arrangement, and mechanical properties on the drag measured in a channel flow.

INTRODUCTION

Soft and hard biofilms that form in marine vessels and vehicles produce undesirable effects such as increased skin friction drag, and degradation of material and performance, as reported in previous studies (Schultz & Swain, 2000; Hartenberger *et al.*, 2020). Predicting the drag produced by soft fouling is challenging due to heterogeneity in growth, lack of material properties to develop models, and sloughing, to name a few. Several studies such as Hutchins *et al.* (2023); Monty *et al.* (2016); Neuhauser *et al.* (2025), etc have addressed drag of heterogeneous roughness distribution. Most of such studies rely on using roughness parameters, such as equivalent sand grain roughness, of constituent elemental roughness to predict the drag of a given distribution. However, using such a methodology to predict the drag of soft fouling is challenging not only due to accurate estimation of roughness parameters of fouling surfaces needed for drag prediction, but also a framework essential to predict the drag of such complex surfaces taking into account distribution and material properties.

Several factors contribute to the lack of availability of roughness parameters of soft fouling. Non-uniform growth and its dependence on flow shear can result in distributions that can be significantly different for the same growth duration. Growth can also result in the presence of protrusions at different spots, as shown in Hartenberger *et al.* (2020), resulting in locally increased form drag, which can skew drag measurements. In addition, not knowing the mechanical properties of such films makes it challenging to develop a model based on distribution characteristics. Finally, sloughing of soft films (Hartenberger *et al.*, 2020) during testing results in drag characteristics that are not consistent in each trial, making repeatability and estimation of skin-friction with *Re* difficult. Given such complications, the use of classical estimates of roughness, such as equivalent sand grain roughness, for a soft fouling colony needs to be revisited in the context of drag prediction.

In this study, we explore the effects of roughness heterogeneity in the drag production of flat plates informed by distributions observed on live fouling, for both hard and compliant synthetic surfaces. We start by detailing the experimental setup in Approach. Next, we introduce the steps followed to generate compliant and rigid synthetic fouling. Next, we present the initial set of heterogeneous roughness distributions, from normal to the flow strips to patchy elements in both hard (sandpaper) and compliant forms (PDMS). The results section introduces the effects on drag of various parameters such as area coverage, surface arrangement or material properties. Finally, we explore the future work to be conducted and presented at the conference.

APPROACH

The main objective of the present study is to identify the role of factors that contribute to the observed drag measurement spread of live fouling (Hartenberger *et al.* (2020)) by considering three aspects of the problem. To address the variation in drag measurements due to coverage and distribution, we vary the arrangement of synthetic biofouling test substrates and study the effect of the total coverage area and distribution. We leverage our current collaboration with NRL-Key West to perform growth studies and corresponding drag of live biofilms at various conditions to understand the relationship between growth properties (distribution, coverage, compliance) and drag. All the results involving live fouling will be included in the final presentation. To eliminate the problem associated with lack of repeatability in experiments involving live fouling, the use of synthetic materials , such as Alginate, and PDMS are used in known distribution and coverage. By using these materials, the effect of material properties (compliance) is studied.

Drag measurements

A recirculating turbulent channel flow setup (Skin Friction Flow Facility (SF3) at University of Michigan) is used to assess the drag characteristics of rough surfaces. The SF3 measures the pressure drop along the channel at ten locations in the streamwise direction Hartenberger *et al.* (2020). The SF3 estimates C_f (skin-friction coefficient) of surfaces mounted on both the top and bottom sides of the fully developed channel flow.

The SF3, which follows a similar approach as the simplified schematics displayed at in Figure 1 is a high-aspect ratio, closed-loop channel flow facility with fully developed turbulent flow in the test-section with a channel height 6 mm, capable of reaching Re_{H} ∼150,000. The SF3 channel gap height, H_0, is nominally 7 mm, span is 101.6 mm, and has a downstream length of 1.14 m. The flow is tripped after passing through honeycombs and mesh screens at the entrance of the channel using an 80-grit sandpaper strip in both facilities. The BSFV measures the skin-friction C_f of surfaces based on the pressure drop across the 10 pressure ports (located at 20H, 30H, 50H, 70H, 84H, 98H, 112H, 126H, 140H, and 150H) along the test-section as shown in figure 1 below. The measurements at each step are averaged after trimming 5 seconds post and pre-transition to another step. The averaged measurements along with the known streamwise port location are used to estimate the pressure gradient dp/dx used in the estimation of the shear stress at the wall. Only measurements acquired in the fully developed turbulent flow region (between 70H and 150H) are used for the pressure gradient estimation. An accurate estimation of the shear stress relies upon the correct dp/dx, and height measurements. The volumetric flow rate, Q, was measured using an ultrasonic flow meter (Omega FDT-25) at the BSFV and a Siemens Sitrans FM MAG5100 magnetic flow meter in the SF3. The temperature is also measured using a Resistance Temperature Detectors (RTD) and logged during data acquisition. Density and kinematic viscosity are obtained as functions of the logged temperature following the ITTC freshwater tables. The bottom window of the SF3 used in conjunction with the rough surfaces is a hydro-dynamically smooth panel with an optically clear fused quartz insert for PIV laser illumination. Simultaneous PIV measurements can be acquired during the pressure data acquisition. All synthetic surfaces, including sandpaper studies, were performed in an asymmetric configuration (rough-smooth) in the SF3. Using the pressure drop measurement, channel height, and mean velocity, the wall shear stress and the skin friction are estimated as follows:

In a fully developed turbulent channel flow like the SF3, the wall shear stress ($\tau_{w,s}$), of either of the two identical top and bottom plates (smooth or rough) is related to the pressure drop ($\frac{dp}{dx}$) as,

$$\tau_{w,s} = \frac{H}{2}\frac{dp}{dx} \tag{1}$$

Here H is the average channel height between the plates, and the pressure drop dp/dx is obtained using a set of pressure taps equally distributed across the streamwise axis of the test section. The suffix 's' denotes a symmetric configuration. The pressure drop was recorded using three different pressure transducers of varying range and resolution. If the top and bottom plates used have similar hydrodynamic roughness characteristics (symmetric roughness about the channel mid-plane), the above relationship can be used to estimate wall shear stress τ_w. In the event of two dissimilar surfaces, one smooth and one rough, asymmetric in wall shear stresses, result in the following relationship for wall shear stress estimation,

$$\tau_{w,a} = H\frac{dp}{dx} - \tau_{\omega,smooth} \tag{2}$$

Several approaches can be performed to acquire $\tau_{\omega,smooth}$. A common methodology relies on flow measurements conducted with Particle Image Velocimetry techniques (PIV) to assess the characteristics of the smooth wall and reconstruct $\tau_{\omega,smooth}$ with a Clauser approach Hartenberger *et al.* (2020); Walker (2014). In our case, the lack of PIV techniques implies that a secondary method must be followed. Using the well-known experimental equation presented by Zanoun *et al.* (2009), we obtain $\tau_{\omega,smooth}$ by assuming a $C_{f,smooth} = 0.074Re_H^{-0.25}$. Here, Re_H is the Reynolds number based on height and can be defined as $Re_H = HU_b/\nu$, with ν representing the dynamic viscosity of the fluid, and U_b representing the bulk velocity.

Upon estimating the wall shear stress, the skin-friction coefficient C_f is calculated using,

$$C_f = \frac{\tau_w}{\frac{1}{2}\rho {U_b}^2} \tag{3}$$

where ρ is the density of the fluid. The density values were adjusted to account for the water type (fresh or saline) and temperature. Upon estimation of τ_w, the overall performance of the plates in terms of drag production is presented as a relative increase or decrease compared to a smooth plate under similar flow conditions (Re_H), and calculated using Zanoun *et al.* (2009). All the results presented as ΔC_f (%) is calculated as follows:

$$\Delta C_f(\%) = 100 \times \frac{C_{f,rough} - C_{f,smooth}}{C_{f,smooth}} \tag{4}$$

Drag measurements from the SF3 have been validated against the expected drag of a smooth plate in a turbulent channel flow reported from the literature.

Developing synthetic configurations to replicate biofouling

To study the effect of arrangement and coverage, the skin-friction drag of rigid-rough and synthetic compliant biofilm-like elements placed on a flat plate was measured.

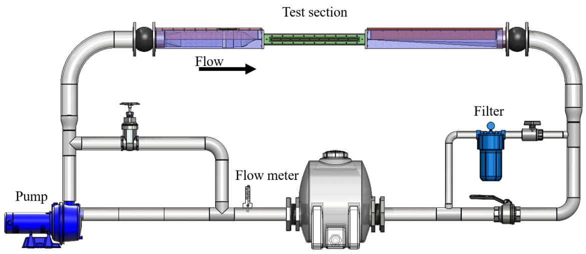

Figure 1. Schematics of a turbulent channel flow facility, similar to the Skin Friction Flow Facility (SF3) used in this study.

Table 1. Test subjects configurations for synthetic fouling experiments.

Plate	Coverage	Material	Protrusion
I, A	0-100%	80 grid	0.9 mm
II, A	5, and 10%	80 grid	0 and 0.9 mm
II, B	5%	80 grid, PDMS	0 mm
III, B	10%	PDMS	0 mm
IV, A	5%	80 grid	0 mm
IV, B	5%	80 grid	0 mm
IV, C	5%	80 grid	0 mm

Rigid roughness elements were constructed from 80-grit sandpaper strips glued to a flat PVC window. The length of the strips is equal to the width (W) of the flow channel, and the width is kept as 5 mm, or $0.7H$. Table 1 details the characteristics of each of the configurations. Synthetic surfaces were developed in collaboration with Professor Jon Estrada's research group at the University of Michigan. Two candidates, alginate, and PDMS, were used to prepare compliant synthetic surfaces, including hydrogels that can interact with water. All synthetic surfaces can be carefully formulated to achieve a range of mechanical properties. The formulation and characterization of these artificial synthetic surfaces are discussed next.

PDMS The first artificial component developed is based on Polydimethylsiloxane (PDMS). This type of component has been used to replicate flexible and compliant materials, and by adequately tuning its components, a vast range of mechanical properties can be achieved Palchesko *et al.* (2012); Wang *et al.* (2020). Due to its compliant nature and tunable mechanical properties, we believe it can be a good candidate to reproduce the properties of live boifilms. Although this element does not have an organic base, its compliant-like properties allow us to use it for our study, and its robustness under flow conditions is beneficial to study compliance in a controlled manner. The PDMS used for the results presented here follows the same conditions presented at Wang *et al.* (2020) ($1:7.5$ gel to mass ratio with a static storage modulus of $E_0 = 158kPa$). In future work, we will explore several blends to analyse the impact of compliance on the drag performance. This manuscript discusses the drag measurements for PDMS surfaces. The authors expect to share results using carrageenan and alginate in the presentation.

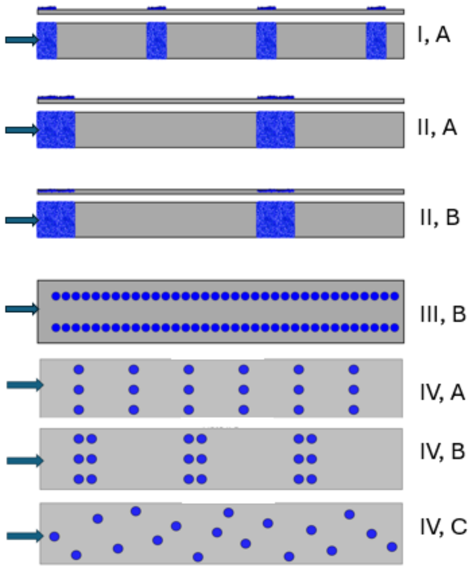

Figure 2. Plates roughness configuration followed in this study.

Roughness configurations

To study the effects of area coverage and surface distribution on the drag of biofilms, we develop several testing plates with varying characteristics, as show at Figure 2. We start by performing drag measurements of plates with heterogeneous roughness made with strips of sand paper. The second approach consists of circular samples made of synthetic fouling on the surface of a flat plate, both in heterogeneous and homogeneous configurations, to replicate the growth of live biofilms.

RESULTS

Drag studies of synthetic surfaces: Effect of surface distribution, area coverage, and material properties

Motivated by appreciable spread observed in drag measurements of live fouling (Hartenberger *et al.* (2020)), the effect of area coverage, including surface arrangement and mechanical properties were investigated using compliant and rigid synthetic surfaces using the SF3 at the University of Michigan to understand how integrated measurements based on pressure drop compare for various configurations. The main motivation was to isolate the effect of the heterogeneity of morphology and topography on the inferred roughness quantities such as k_s^+. Here, we start by conducting drag measurements on flat plates with streamwise heterogeneity made of strips of sandpaper and PDMS. We analyze the effects of varying the area coverage and the distribution arrangement around the plate. The effect of material compliance on a given area coverage and distribution will be discussed next. The following subsections discuss the synthetic surfaces study for rigid roughness and PDMS.

Testing configurations The configuration of the plates followed here is presented in Figure 2 and shown in Table 1

Plate I presents equally spaced streamwise roughness for different coverage ratios. To increase the coverage, an extra roughness strip is placed in between two existing ones. Plate II follows the same approach, but the roughness bands are twice as wide as for Plate I, and the spacing is also doubled. Plate III consists of equally spaced circles in a streamwise arrangement. In configuration A, the roughness bands are protruding into the flow, and in arrangement B, the elements are flush with the surface. Plate IV A, B and C cover a second approach involving patchy distributions for a similar coverage at three different configurations, from normal to the flow rows, to a quasi-random arrangement at Plate IV, C. The details can be found at Table 1

Effect of area coverage: Rigid roughness

The effects of area coverage are presented in the top-left panel of Figure 3. The roughness distribution of Plate I, A is increased by adding extra roughness strips in between existing ones, while keeping the streamwise distance between lines constant for a given area coverage. As expected, the drag penalty increases with area coverage, but not linearly. While 100% coverage yields maximum drag penalties, we observe that a mere 5% is producing almost half the drag of the fully covered case. The extra form drag added by the encounters between the flow and the spanwise obstacles can be responsible for this. A 10% coverage area (Plate I, A, as depicted at Figure 2) provides almost 80% drag penalty compared to the 100% plate.

Effect of surface distribution: Rigid roughness with and without protrusion

To evaluate the arrangement effects, we prepare a second plate, where the width of the strips, when compared to Plate I, A is doubled. Plate II, A presents the same coverage area, but the distance between obstacles doubles. The results are introduced in the top-right panel of Figure 3. For this new case, we observe that the drag penalty increase when the coverage area goes from 5 to 10% is not as prominent as with Plate I, A, further highlighting the importance of form drag, number of obstacles, and roughness strip width. When comparing Plate I and II at equivalent coverage ratios, we observe that Plate II promotes a drag increase for a comparable coverage ratio of 30% less than Plate I, highlighting the relevance of distribution on drag performance. Area coverage alone can not be used as a predictive parameter for overall drag when other aspects (heterogeneity, protrusion height) are present. To further explore this, we prepare a new plate, Plate II, B. The distribution of the rough elements is similar to Plate II, A, but the roughness strips are flush with the surface. The results are shown in the bottom-left panel of Figure 3 As expected, and for a coverage of 5%, reducing the protrusion height has an immediate effect on the drag and lowers the penalty considerably. Still, this scenario of a "flush roughness" is unrealistic for actual biofouling approaches, and is explored here just for validation purposes.

Effect of mechanical properties and distribution for a compliant material (PDMS)

To further explore the effects of mechanical properties on fouling, we prepared a compliant version of Plate II, B. In this case, the sandpaper strips are replaced by PDMS with a 7.5:1 mixture ratio (see methodology for more details). The results, introduced in the bottom-right panel of Figure 3 suggests that replacing synthetic hard biofouling with a soft, compliant alternative reduces the drag penalty by almost 50%. This result further reinforces the idea that the mechanical properties and topology of biofouling are major players in explaining and predicting the drag associated with fouled surfaces.

To summarize the preliminary findings presented before, we prepare Plate III. In this case, the streamwise strips are replaced by circular clusters, following an approach more consistent with the way biofouling forms, although in a highly simplified way. Plate III (PDMS) B follows an area coverage of 10%, while Plate II, B (PDMS) coverage is reduced to 5%. Still, as seen at the bottom-right panel of Figure 3, the latter shows a higher drag penalty value. With this simplified study, evidence point towards factors to be incorporated for predicting the drag produced by biofouling. A better understanding needs to be achieved on how each of the roles explored here (area coverage, surface distribution, protrusion height, and mechanical properties) interacts with the others, since taking them as isolated contributors will yield unreliable predictive models.

Effect of patchy roughness distributions on drag production

In this final section, the roughness texture are built following a patchy heterogeneous distribution over the surface of the flat plate. As shown at figure 2, we place circular elements made of sandpaper in several distributions along the surface. The diameter of the elements corresponds to two times the empty height of the flow tunnel ($2H$). We start with two plates where the elements are arranged in rows normal to the flow. In this case, similar to the plates with strips presented before, no noticeable differences in the drag penalty are observed. It will be a matter of further studies to analyse if this similar drag production remains when the samples are protruding into the flow. Still, when a new quasi-random distribution is incorporated, the variance starts to display again, as the new configuration, Plate IV, C produces roughly 10% less drag penalty than the other two plates. This finding highlights the importance of area arrangement when analysing roughness textures. For comparison, we present an equivalent drag penalty by calculating the 5% drag generation of a plate fully covered by 80 grit sand paper, showing that, when roughness is heterogeneous and patchy, a linear interpolation based on area coverage % is not enough to properly predict drag, as seen by the larger penalty developed by Plates VI in all three configurations.

Biologically derived synthetic materials under consideration.

Carrageenan is a component extracted from seaweed that can produce water-based hydrogels Therkelsen (1993). By controlling the concentration of the material in the dissolution and immersion time in water, hydrogels with various strengths can be extracted. Figure 5(a) presents a set of mechanical properties tests conducted for carrageenan-based hydrogels of concentration ranging from 1 to 2.5% and submersion time ranging from 0 to 48h. The samples are made by mixing water and carrageenan at constant stirring (300 rpm) and 90 $^\circ$ C for 3 hours, with an extra hour under no stirring for the mixture to set (while keeping the temperature). Then, the samples are cast into molds and left for a day at 4 $^\circ$ C. The mechanical properties measurements are obtained using a Dynamic Mechanical Analysis (DMA) tool, and consist of steady and dynamic cases. The steady set involves compression at a constant velocity, where the deformation is recorded (left column, Figure 5 (a)). The second set corresponds to a dynamic amplitude sweep test, where the deformation is applied in a sinusoidal form (compression-relaxation), and the amplitude is increased under a constant frequency. The results suggest that larger concentrations of the sample provide stronger hydrogels, as observed by the steepness of the deformation vs

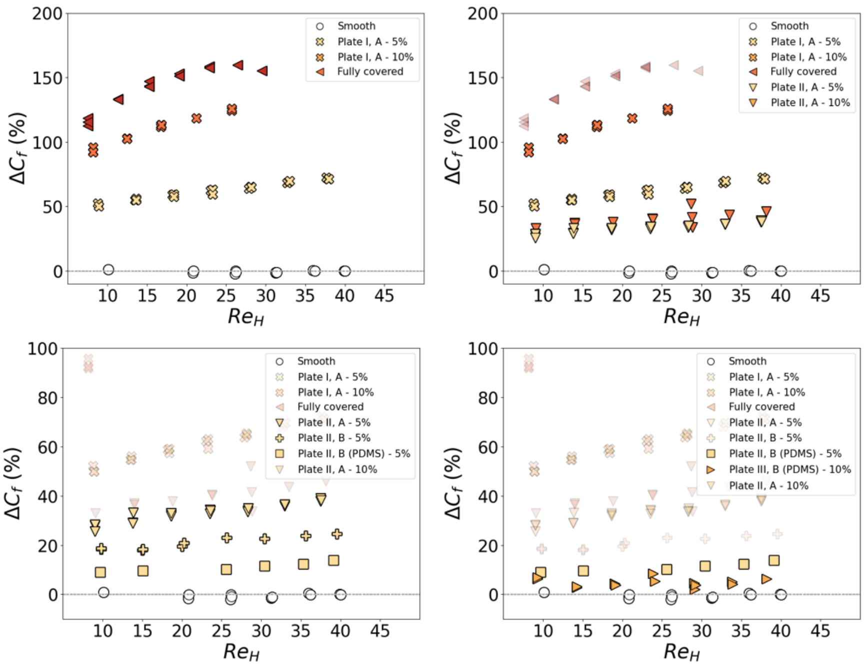

Figure 3. Drag increase (compared with a smooth plate) vs Re_H $(\times 10^-3)$ for plates with synthetic roughness. Top-left panel: area coverage study. Top-right panel: surface arrangement analysis. Bottom-left panel: protrusion height and mechanical properties comparison. Bottom-right: compliant material under various arrangements.

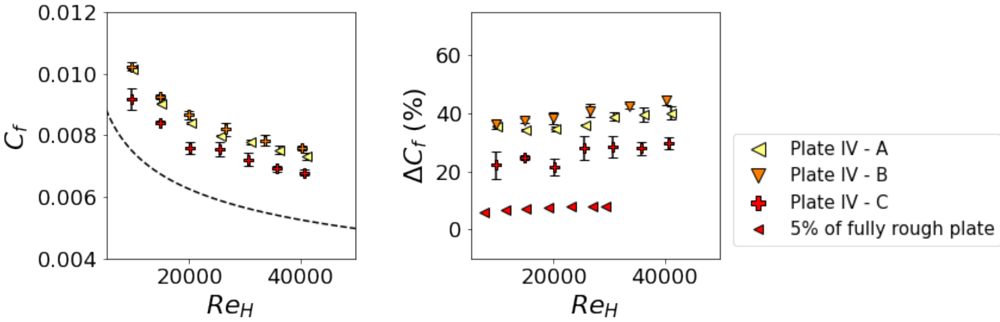

Figure 4. C_f and Drag increase (compared with a smooth plate) vs Re_H for plates with synthetic roughness. left panel: C_f for all plates under Plate IV arrangement. right panel: ΔC_f [%] for all plates under Plate IV arrangement with respect to a theoretical smooth plate (black-dashed line at the left panel). Red triangles show 5% of the drag penalty produced by a plate fully covered by 80 grit sandpaper.

stress curve. Water submersion time weakens the samples and reduces their mechanical strength. Although preliminary testing shows that carrageenan samples are largely degraded under water shear, preventing us from using them as reliable candidates for live fouling replicas, the possibility of controlling that degradation make them suitable choices for sloughing analysis, and it will be considered in future work.

Alginates are polysaccharides isolated from brown algae such as *Laminaria hyperborea andlessonia* found in coastal waters around the globe Augst *et al.* (2006). Our samples are developed using the double crosslinking method proposed by Ji *et al.* (2022). First, a weak hydrogel is formed with a mixture of sodium alginate with a total weight concentration of 2% and a $CaSO_4$ solution of 0.3%. The mixture is stirred at 300 rpm at room temperature for a duration of 3 hours and then placed in vacuum to remove the air. This procedure helps to hold the shape of the hydrogel, and creates an initial weak specimen, with a semi-transparent appearance. After curing at 4° C for one day, the samples are immersed in a $CaCl_2$ bath with a molarity of 0.1M for another day to enhance the mechanical strength of the samples. The differences after the cross-linking method are highlighted by the amount of calcium in the overall hydrogel, represented by the white color, in contrast to the transparent appearance of the original surface (figure 5 (b)). The external crosslinking bath greatly enhances the mechanical capabilities of the hydrogel Ji *et al.* (2022). Preliminary testing show that alginate-based hydrogels are able to withstand water shear forces for 30 minutes under 5m/s. Hence, their use as replicas for live fouling will be explore further. As shown next, we have been able to develop compliant equivalents of 80 grit sandpaper, which will further complement the analysis presented in this paper.

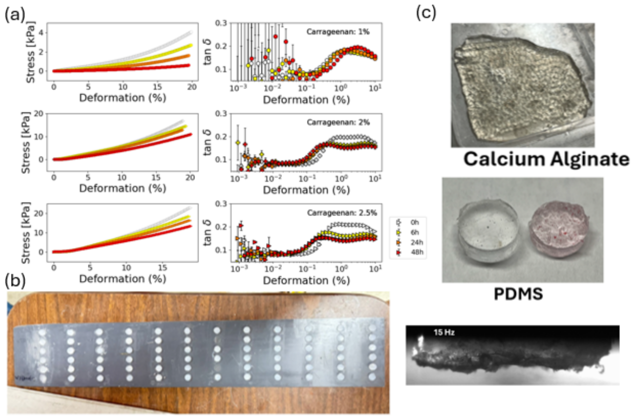

Figure 5. (a) Mechanical properties analysis of the carrageenan-based samples. The left column presents the results obtained during the stress-deformation testing. The right column introduces a dynamic testing, where the amplitude of deformation is increased at a constant frequency (f=1Hz). The figure reports the deformation against the loss factor (tan δ). (b) Plate covered with alginate-base samples. (c) Compliant-roughness preparations of PDMS and calcium alginate. Bottom figure of right column show one of those patches under incoming flow velocity.

CONCLUSIONS AND FUTURE WORK

In this work, we have analysed how parameter such as area coverage, surface arrangement, protrusion height, and texture properties play an important role of the drag produced by a flat plate in a turbulent channel flow. By systematically varying the mentioned parameters, it has been discussed how discrepancies in drag production, when assessed with respect to a smooth plate, arise, even for test subjects where some of those aspects are equal. As future work, we'll take one step further and study the impact of compliant rough elements that better describe the unsteady nature of soft biofouling in terms of protrusion height. Replicas of sandpaper are developed using PDMS and alginate, and their drag impact for several coverage ratios, surface distributions, and mechanical properties will be analysed. We will use the results obtained during the live fouling testing at NRL Key West to inspire distributions around the plate that mimic the growth of real biofouling. The final presentation will show how, under certain conditions, live seawater biofilms follow the heterogeneous patchy arrangement prescribed here, and will present its effects on drag production and spread.

ACKNOWLEDGMENTS

We thank the ONR-funded Center for Naval Research and Education (CNRE) at the University of Michigan for supporting Dr. Vilumbrales-Garcia. We acknowledge the support from Bhumi Kumar, Chelsea Sun, Sameer Kheterpal, Elliot Scully, and Joseph Beckett.

REFERENCES

Augst, Alexander D, Kong, Hyun Joon & Mooney, David J 2006 Alginate hydrogels as biomaterials. *Macromolecular bioscience* **6** (8), 623–633.

Hartenberger, Joel D, Callison, Elizabeth G, Gose, James W, Perlin, Marc & Ceccio, Steven L 2020 Drag production mechanisms of filamentous biofilms. *Biofouling* **36** (6), 736–752.

Hutchins, N, Ganapathisubramani, B, Schultz, MP & Pullin, DI 2023 Defining an equivalent homogeneous roughness length for turbulent boundary layers developing over patchy or heterogeneous surfaces. *Ocean Engineering* **271**, 113454.

Ji, Donghwan, Park, Jae Min, Oh, Myeong Seon, Nguyen, Thanh Loc, Shin, Hyunsu, Kim, Jae Seong, Kim, Dukjoon, Park, Ho Seok & Kim, Jaeyun 2022 Superstrong, superstiff, and conductive alginate hydrogels. *Nature Communications* **13** (1), 3019.

Monty, JP, Dogan, E, Hanson, R, Scardino, AJ, Ganapathisubramani, B & Hutchins, N 2016 An assessment of the ship drag penalty arising from light calcareous tubeworm fouling. *Biofouling* **32** (4), 451–464.

Neuhauser, Jonathan, Schmidt, Carola, Gatti, Davide & Frohnapfel, Bettina 2025 Predicting the global drag of turbulent channel flow over roughness strips. *International Journal of Heat and Fluid Flow* **115**, 109848.

Palchesko, Rachelle N, Zhang, Ling, Sun, Yan & Feinberg, Adam W 2012 Development of polydimethylsiloxane substrates with tunable elastic modulus to study cell mechanobiology in muscle and nerve. *PloS one* **7** (12), e51499.

Schultz, Michael P & Swain, Geoffrey W 2000 The influence of biofilms on skin friction drag. *Biofouling* **15** (1-3), 129–139.

Therkelsen, Georg H 1993 Carrageenan. In *Industrial gums*, pp. 145–180. Elsevier.

Walker, Jessica M 2014 The application of wall similarity techniques to determine wall shear velocity in smooth and rough wall turbulent boundary layers. *Journal of Fluids engineering* **136** (5), 051204.

Wang, Jin, Koley, Subhra Shankha & Katz, Joseph 2020 On the interaction of a compliant wall with a turbulent boundary layer. *Journal of Fluid Mechanics* **899**, A20.

Zanoun, El-Sayed, Nagib, Hassan & Durst, Franz 2009 Refined cf relation for turbulent channels and consequences for high-re experiments. *Fluid dynamics research* **41** (2), 021405.